Progress Report on Radiation Dosimetry Standards at NMIJ/AIST

Norio Saito, Tadahiro Kurosawa, Masahiro Kato,
Yuichiro Morishita, Akihiro Nohtomi and Nobuhisa Takata
Ionizing Radiation Section, Quantum Radiation Division
National Metrology Institute of Japan (NMIJ)
National Institute of Advanced Industrial Science and Technology (AIST)
Tsukuba 305-8568 Japan

1. Introduction

Ionizing Radiation Section in NMIJ/AIST provides the X-rays, γ-ray, and β-ray standards in Japan as a primary NMI. We provide air kerma rate of X-rays and γ-rays, and photon intensity of monochromatized synchrotron radiation in the soft X-ray region. Recently, we established the primary standards for absorbed dose rate to tissue for beta particles emitted from Sr-90/Y-90, Kr-85 and Pm-147 radionuclide. We are developing the absorbed dose to water for γ-rays from ^{60}Co and the dose equivalent for X-rays and γ-rays. We performed the key comparison of medium-energy (BIPM.RI(I)-K3) and low-energy (BIPM.RI(I)-K2) X-rays with BIPM in September 2006.

2. Standards for gamma rays

2-1. Air kerma standards

Air kerma standards for ^{60}Co and ^{137}Cs gamma rays at NMIJ were peer-reviewed in December 2003 and ISO17025 quality system was established in 2004. The range of air kerma rate and calibration and measurement capability (k=2) are listed in Table 1.

Table 1 Range of air kerma rate and calibration and measurement capability (k=2)

Source	Range of air kerma rate (Gy/s)	Calibration and measurement capability (k=2)
^{60}Co γ-rays	2.0×10^{-9} ~ 4.3×10^{-2}	1.0 % at 1.3×10^{-2} Gy/s
^{137}Cs γ-rays	6.1×10^{-10} ~ 4.6×10^{-4}	0.8 % at 6.6×10^{-4} Gy/s

2-2. Absorbed dose to water of ^{60}Co Gamma rays

A graphite calorimeter is being developed for the absorbed dose to water of ^{60}Co. We will measure absorbed dose to water using it in next year and plan to start the calibration service in 2009.

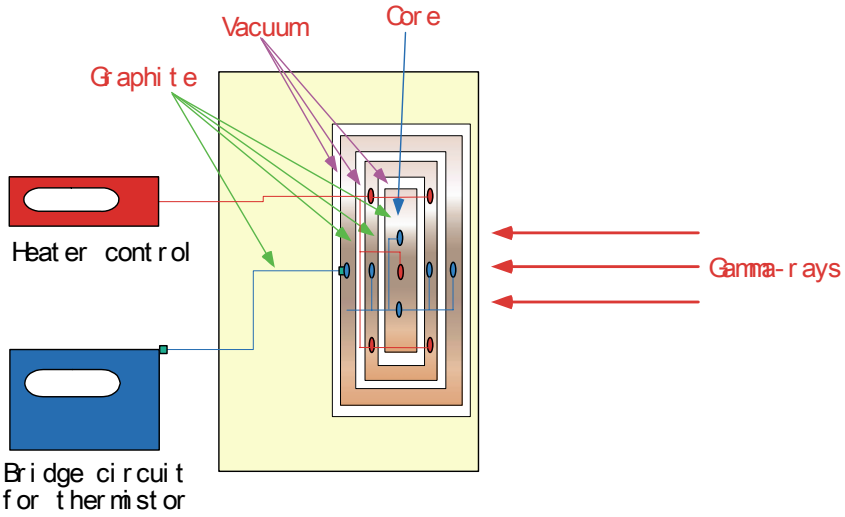

Figure 1 Schematic diagram of our graphite calorimeter.

2-3. Evaluation of dose equivalent

For the estimation of dose equivalent H*(10) and Hp(10), we will measure the energy spectra for ^{60}Co and ^{137}Cs irradiation fields using a Ge detector. The response functions of our Ge detector were evaluated by using the EGS code. We finished the spectra measurements and we will start the calibration service of H*(10) and Hp(10) in this year.

3. Standards for medium-energy X-rays

3-1. Air kerma standards for medium-energy X-rays

Air kerma standards for medium-energy X-rays at NMIJ were peer-reviewed in February 2005, and ISO17025 quality system was established in June 2005. The range of air kerma rate and calibration and measurement capability (k=2) are listed in Table 2.

Table 2 Range of air kerma rate and calibration and measurement capability (k=2)

Source	Range of air kerma rate (Gy/s)	Calibration and measurement capability (k=2)
Medium energy X-rays (40~300 kV)	9.0×10^{-9} ~ 2.0×10^{-3}	1.2 % at 2.7×10^{-4} Gy/s

The qualities of X-rays provided are BIPM quality, Narrow spectra (ISO4037) and Japanese QI (quality index, E_{eff}/E_{max}), where E_{eff} is the effective X-ray energy and E_{max} the maximum X-ray energy. We are now preparing air kerma standards for the X-ray qualities of ISO 4037.

3-2. Correction factors from the aperture

We re-evaluated correction factors [1] relating to scattering (K_{sd}) and transmission (K_{tr}) of incident X-rays at an aperture of our free-air ionization chamber using the computational Monte Carlo code (EGS5). The squares in Figure 2 show the products of K_{sd} and K_{tr} when mono-energetic X-rays (50-250 keV) collide with our aperture which is 10 mm in diameter and 20 mm in thick. These results were compared with those evaluated with the other simulation code (MCNP) [1], which is shown with the circles in Figure 2. The simulated correction factors by the different codes agreed with each other within 0.1 %. Then we simulated the correction factors for different aperture angles to minimize the correction. The aperture angle is defined as described in the Figure 3. The computed results for aperture angles from -2 to 2 degrees are shown in Figure 3. It was found that the aperture of zero degree (currently used in AIST) minimizes the correction factor, and the corrections increase as the aperture angle gets larger for both positive and negative directions.

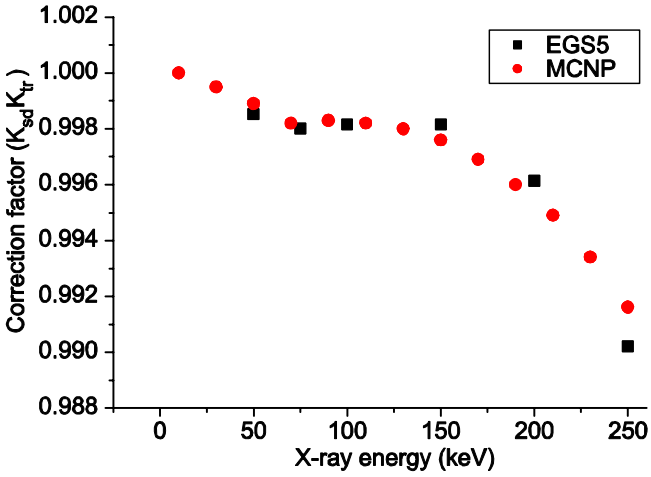

Figure 2 Products of K_{sd} and K_{tr} for mono-energetic X-rays.

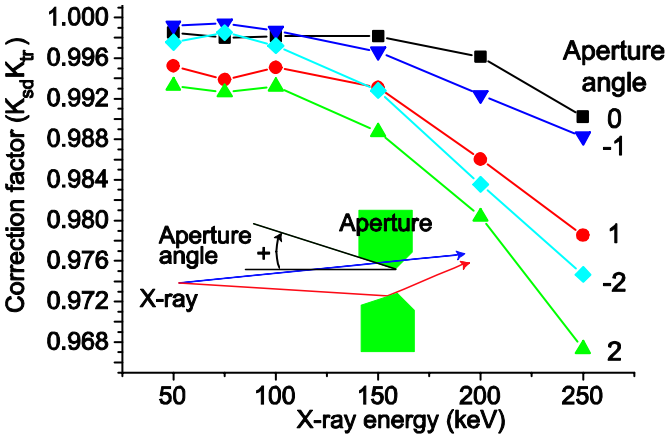

Figure 3 Angle dependences of correction factors ($K_{sd}K_{tr}$).

3-3. Key comparison with the BIPM

We made a key comparison with the BIPM (BIPM.RI(I)-K3). The comparison was performed using three different transfer chambers (A2 and A3 by EXRADIN and 30013 by PTW) irradiated by the BIPM qualities at 250, 180, 135 and 100 kV. To do so, we newly established the BIPM qualities referring to Ref. [2].

3-4. Contribution from scattered photons

Calibration coefficients are considered to be influenced by contribution of scattered photons due to the different size of a collimator and filters. This contribution depends on irradiation apparatus. We have estimated the contribution of the scattered photons in the

calibration for the BIPM quality. We performed the following experiments, so called as a shadow method. The experimental setup is illustrated in Fig.4 and a photograph is shown in Fig.5.

1. We measure the signals from the free air chamber and an ionization chamber without the stopper.
2. We measure the signals from the free air chamber and an ionization chamber with the stopper.

The difference between the signals with and without the stopper is the contribution of the scattered photons. The experiments yield that the contributions of the scattered photons for ionization chambers are larger than those for the free air chamber. The difference between the contributions of the scattered photons for the free air chamber and the ionization chamber should be corrected.

We took a distribution of X-ray beam using an imaging plate shown in Fig.6. This picture clearly displays that there are the scattered photons in the shadow region.

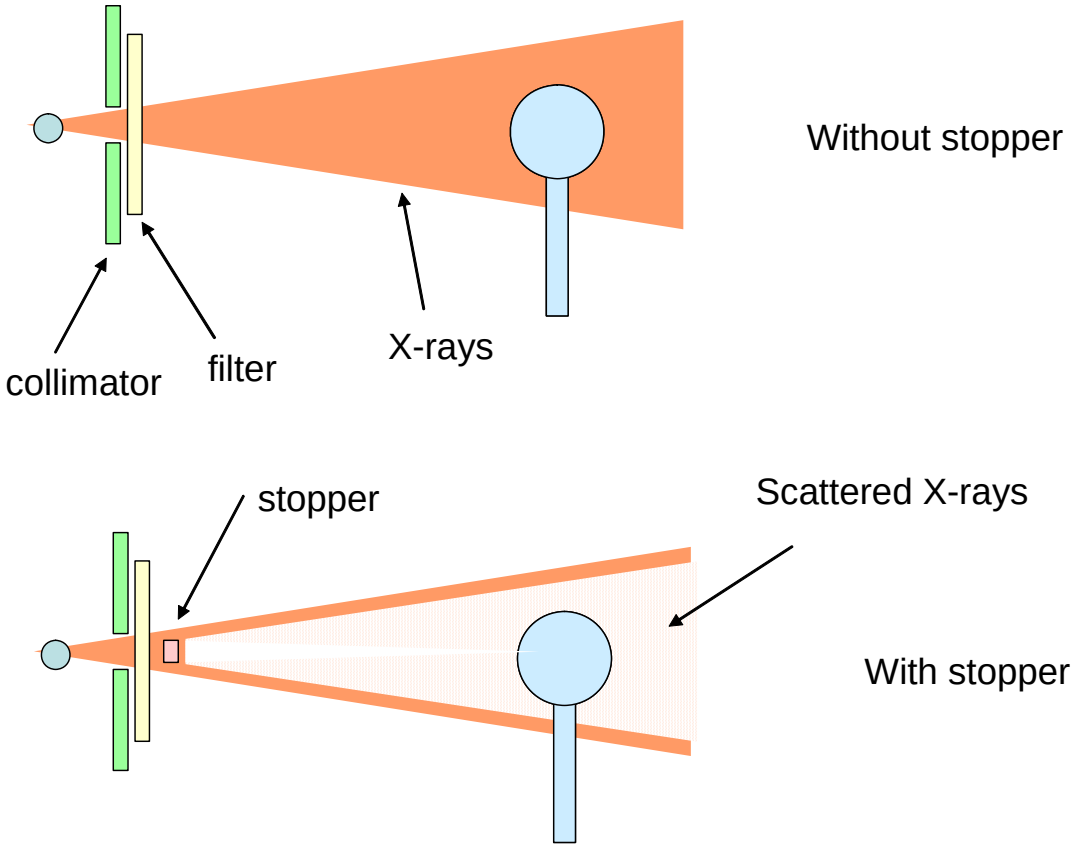

Figure 4 Experimental setup

Figure 5 Photograph of the stopper setting

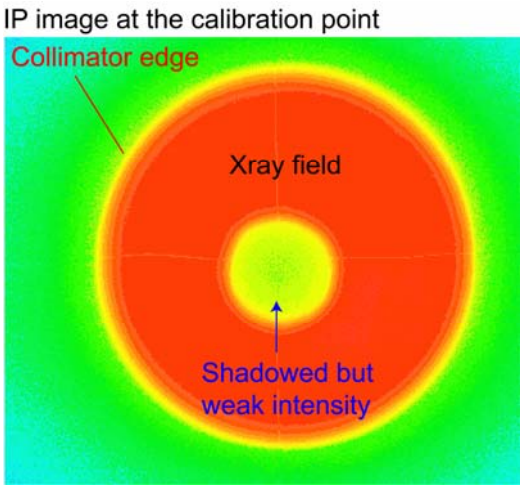

Figure 6 Distribution of X-ray beam inserted with the stopper measured with an imaging plate.

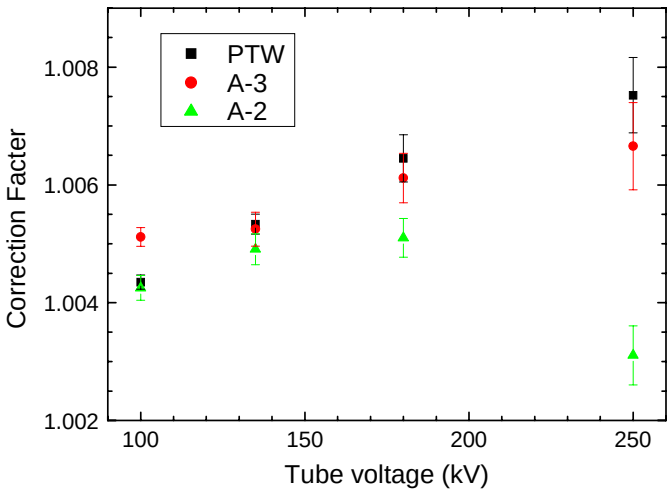

Figure 7 Correction factors for the scattered photons for the three ionization chambers.

The results are shown in Fig.7. The correction factors depend on the x-ray quality, the size of the ionization chamber. The standard deviation of the measured correction factors is less than 0.1%.

4. Standards for low-energy X-rays

4-1. Air kerma standards for low-energy X-rays

Air kerma standards for low-energy X-rays at NMIJ were peer-reviewed in February 2005, and ISO17025 quality system was established in June 2005. The range of air kerma rate and calibration and measurement capability (k=2) are listed in Table 3.

Table 3 Range of air kerma rate and calibration and measurement capability (k=2)

Source	Range of air kerma rate (Gy/s)	Calibration and measurement capability (k=2)
Low energy X-rays (10~50 kV)	2.5×10^{-6} ~ 1.0×10^{-2}	0.7 % at 4.4×10^{-5} Gy/s

4-2 Field-size effect on the calibration

The contribution of scattered X-rays in dosimetry measurements is estimated using a parallel-plate ionization chamber and a spherical ionization chamber for low energy X-rays by changing the field-size of the radiation. We obtained the correction factors for the field-size effect [3].

4-3. Evaluation of the dose equivalent

Recently, we directly measured energy spectra of X-rays by means of a high resolution Schottky CdTe detector for various radiations qualities (Figure 8). The obtained data enabled us to evaluate the dose equivalent H (Sv).

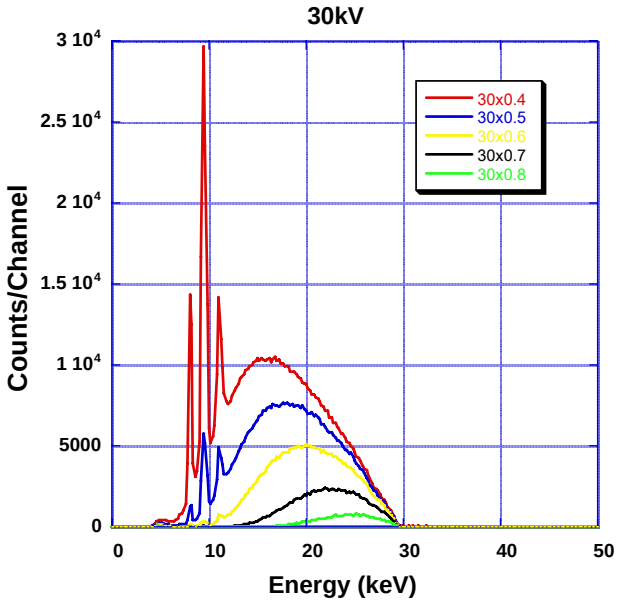

Figure 8 Energy spectra of X-rays obtained from the W-anode X-ray tube for different radiation qualities with the tube voltage of 30 kV.

4.4 Mammographic radiation quality

We will install an X-ray tube with Mo target in this July. We will establish the standards on mammographic radiation quality in this year.

4-5. Key comparison with the BIPM

We performed the direct key comparison with BIPM in November 2004 and the indirect key comparison in September 2006 (BIPM.RI(I)-K2). The indirect comparison was performed using two different transfer chambers (PTW 23344 and EXRADIN A3) irradiated by the BIPM qualities at 10, 25, 30, 50a and 50b kV. The results of the comparisons showed the deviation less than ~0.2% for the direct comparison and ~0.4%

for the indirect comparison.

5. Absorbed dose standards for beta-particle radiation

We have established the primary standards for absorbed dose rate to tissue for beta particles emitted from Sr-90/Y-90, Kr-85 and Pm-147 radionuclide. Beta Secondary Standard 2 (BSS2) is used for producing Series 1 reference beta particle radiation fields described in ISO 6980 (Fig. 9). The absolute values of the absorbed dose rate to tissue at a depth of 0.07 mm are determined by an extrapolation chamber. The absorbed dose rate to tissue and calibration and measurement capability (k=2) are listed in Table 4. We have started the calibration service in September 2006. We have joined in EUROMET project No. 739. We calibrated a transfer chamber used in the project in the beta reference fields. We have plans to perform bilateral mutual comparison with KRISS in 2007.

Table 4 The absorbed dose rate to tissue and calibration and measurement capability.

	Reference absorbed dose rate (Gy/s)	Uncertainty (k=2)
^{90}Sr/^{90}Y with a beam flattening filter at the distance of 30 cm	1.1×10^{-5}	2.8 %
^{85}Kr with a beam flattening filter at the distance of 30 cm	3.8×10^{-5}	2.8 %
^{147}Pm with a beam flattening filter at the distance of 20 cm	2.0×10^{-6}	4.8 %

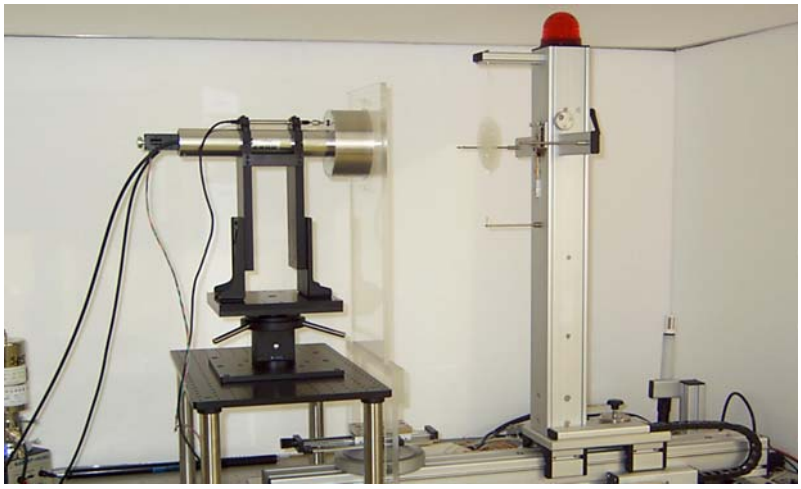

Figure 9 An extrapolation chamber and a beta-ray irradiation system.

6. Radiometry Standards using synchrotron radiation from 0.1 to 4 keV

We started calibration service of photon intensity (photons/s) or power (W) of monochromatized soft X-rays (0.1~1 keV, 1~10nm) using a multi-electrode ionization chamber (Fig.10) [4] with low pressure gas (~0.1 Pa) and synchrotron radiation from 2005. The uncertainty is estimated to be 5-15 % (k=2). Now we are developing a cryogenic substitution radiometer (Fig.6) in the energy region of 0.1-4 keV [5-7]. The uncertainties are achieved to be 1% (k=2) at the photon energy of 0.5 keV and of 0.4% (k=2) at 3.0 keV. A typical example of the cavity temperature as a function of time lapse at 3.0 keV is shown in Fig.11. The temperature of the cavity rose by the amount of 41.56 mK in about 1 minute and then became steady, exhibiting a fluctuation smaller than 0.1 mK. This temperature rise corresponds to the radiant power of 7.57μW. Using this radiometer and the multi-electrode ionization chamber, the photon W-values of dry air are precisely determined in the region of 2-4 keV [7].

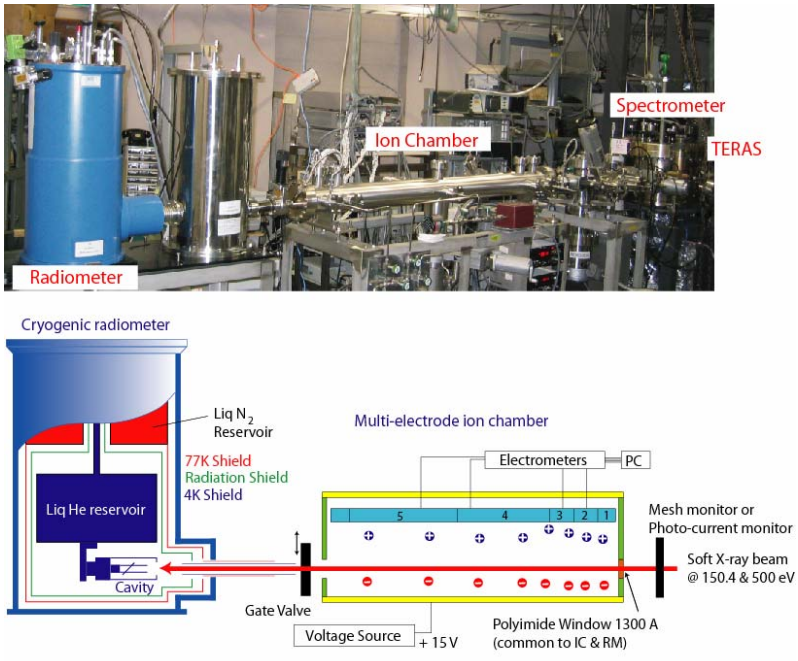

Figure 10. Photograph and schematic figure of the ionization chamber and the cryogenic radiometer.

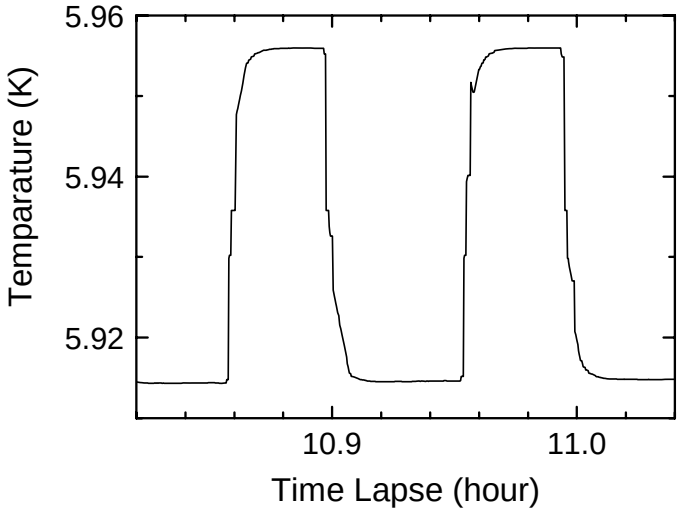

Figure 11 An example of the cavity temperature as a function of time lapse at the photon energy of 3.0 keV.

1. T. Kurosawa and N. Takata, “Correction factors for free-air ionization chambers for X-rays transmitted through a diaphragm edge and scattered from the surface of the diaphragm aperture”, CCRI(I)/05-27 (2005).
2. P. J. Allisy-Roberts et.al., Rapport BIPM-2004/17
3. A. Nohtomi, N. Takata and T. Sakae, “Response of Ionization Chambers for Different Radiation Field-size at Low Energy X-ray Region”, Japanese Nuclear Science and Technology **44**, 1-5 (2007)..
4. N.Saito and I.H.Suzuki, “Absolute fluence rates of soft X-rays using a double ion chamber”, Journal of Electron Spectroscopy and Related Phenomena, **101-103**, 33-37 (1999).
5. Y. Morishita, N. Saito, and I. H. Suzuki, “Comparison of the absolute soft X-ray intensity between a cryogenic radiometer and an ion chamber”, J. Electron Spectrosc. Relat. Phenom. **144-147**, 1071 (2005).
6. M. Kato, A. Nohtomi, Y. Morishita, T. Kurosawa, N. Arai, I. H. Suzuki and N. Saito, “Development of the Soft X-ray Intensity Measurement with a Cryogenic Radiometer”, AIP conference proceedings, **879**, 1133 (2006).
7. M. Kato, I. H. Suzuki, A. Nohtomi, Y. Morishita, T. Kurosawa, N. Saito, “Photon W-value of dry air determined using a cryogenic radiometer combined with a multi-electrode ion chamber for soft X-rays”, submitted.